Journal of Physics: Conference Series **443** (2013) 012011 doi:10.1088/1742-6596/443/1/012011

# What we can learn from magnetic Compton scattering: application to the determination of spin polarization

**J.A. Duffy**

Department of Physics, University of Warwick, Coventry, CV4 7AL, UK

E-mail: j.a.duffy@warwick.ac.uk

**Abstract.** Studies of spin-resolved electron momentum densities involve the measurement of the so-called magnetic Compton profile. This is a one-dimensional projection of the electron momentum distribution of only those electrons that contribute to the spin moment of a sample. The technique is applicable to ferri- and ferromagnetic materials. The profile is obtained via the inelastic 'Compton' scattering of high energy X-rays. Since electrons originating from different atomic orbitals have specific momentum densities, it is often possible to determine the origin of the magnetism present. Typically, interpretation requires the use of electronic structure calculations using molecular orbital and band structure approaches. Here, we highlight the application of the technique to the determination of the Fermi level spin polarization, the knowledge of which is important to the development of novel spintronic materials.

## 1. Introduction to magnetic Compton scattering

Compton scattering studies involve the non-resonant inelastic scattering of high energy photons. Two specific applications of the technique are the measurements of Fermi surfaces and spin resolved electron momentum densities. Incident photon energies of 90-200keV are normally used, and, for magnetic measurements, a degree of circular polarization is required. In order to meet these requirements, the experiments are usually performed at the ESRF and SPring-8 synchrotron X-ray sources.

When the X-rays are inelastically scattered by the electrons in the sample, the scattered photon energy distribution is Doppler broadened because of the electrons' momentum distribution. If the scattering event is described within the impulse approximation [1, 2], the measured spectrum represents a 1-dimensional projection of the electron momentum distribution, $n(\mathbf{p})$, resolved along the $z$ direction, which is parallel to the scattering vector. This is the Compton profile:

$$J\left(p_z\right) = \iint n\left(\mathbf{p}\right) dp_x dp_y, \tag{1}$$

where the integral of $J(p_z)$ is taken over occupied electron states.

Fermi surface studies typically involve an incident monochromatic photon energy of around 90keV. The high X-ray energies used in the experiments mean that the bulk electronic structure is measured. The method requires a high-resolution energy dispersive measurement in order to obtain the momentum resolution necessary to resolve Fermi surface features.

Examples of such studies include the superconductors $La_{2-x}Sr_xCuO_4$ [3], $Na_xCoO_2.yH_2O$ [4] and $Ba(Fe_{1-x}Co_x)_2As_2$ [5]. Whilst several methods are widely used for Fermi surface measurements (including the closely-related positron technique [6]), there are a number of circumstances where Compton scattering is the technique of choice. Positron annihilation, for example, requires a very low defect concentration, and can suffer from positron-electron correlation effects [7]. Quantum oscillatory methods require long electronic mean-free-paths, and photoemission is inherently surface sensitive.

If the incident photon beam has a component of circular polarization, the scattering cross-section contains a term which is spin dependent [8]. This term may be isolated from the charge scattering by either flipping the direction of the sample magnetization or the photon helicity parallel and antiparallel with respect to the scattering vector, resulting in a *magnetic* Compton profile (MCP), $J_{mag}(p_z)$. This MCP is defined as the 1D projection of the spin-polarized electron momentum density:

$$J_{mag}\left(p_z\right) \;=\; \iint \left[\; n^{\uparrow}\left(\mathbf{p}\right) \;-\; n^{\downarrow}\left(\mathbf{p}\right) \;\right] dp_x dp_y. \tag{2}$$

Here $n^{\uparrow}(\mathbf{p})$ and $n^{\downarrow}(\mathbf{p})$ are the momentum densities of the majority and minority spin bands. Since the MCP is the difference between two measured Compton profiles, components arising from spin-paired electrons cancel, as do most sources of systematic error. Because only those electrons that contribute to the spin moment of the sample contribute to the integral of this MCP, it is then possible to determine the spin magnetic moment, usually by comparison with a measurement, under the same experimental conditions, of a sample with known spin moment. Such straightforward spin magnetometry has, for example, permitted the clarification of the temperature dependence of the spin and orbital moments in magnetite [9].

Crucially, from more detailed analysis, it is normally possible to determine the origin of the spin moment via comparison with calculated profiles. This is because electrons in different orbitals have different momentum density distributions: more localised electrons (for example the 4f contribution to the magnetism in Gd) have a correspondingly broad contribution whereas more itinerant electrons have a narrower momentum density distribution. This has been illustrated clearly in materials such as Gd [10], GdY [11], the magnetocaloric material $Gd_3Pd_7$ [12] and the ferromagnetic superconductor $RuSr_2GdCu_2O_8$ [13], where the itinerant 5d contribution is clearly observable in addition to the localised 4f moment. Such an approach can also be applied to 4f-3d systems again because the 3d electrons have a narrower momentum density distribution, as demonstrated in $SmMn_2Ge_2$, where the 4f and 3d spin moments were isolated [14]. Here, the total spin moment approaches zero, but the measurement revealed this to arise from large antiparallel Sm 4f and Mn 3d contributions. Here, the ability to differentiate between the 4f and 3d contributions, together with the sensitivity to only the spin moment, also revealed a subtle field dependence of the individual moments even when the bulk magnetisation was constant [15].

Electronic structure calculations are particularly useful for the interpretation of magnetic Compton profiles. Direct predictions of the MCPs can be made by calculating the resultant spin-dependent momentum distributions. For example, in Ni, as has been described by Dixon *et al.* [16], the experimental results measured along four crystallographic directions provided a stringent test of three different calculations. In such metals, features associated with the Fermi surface arising from bands crossing the Fermi level may be clearly visible. In this case, the theory generally reproduced the experimental results well, with good agreement with the experimental spin moment, and consistency with the Fermi surface features that were observed. However, the results demonstrated a characteristic problem with the *ab initio* calculations: there is a distinct discrepancy at low momentum, where the theoretical results typically overestimate the spin density. This problem is related to the precise location of the spin-polarized bands

relative to the Fermi level. Because in the band structure there is a marked energy dependence of the density of states (DOS) at the Fermi level, very small changes in the calculation have a significant effect on the resultant spin density. It has been demonstrated previously [17, 18], that the agreement with experiment may be optimised by rigidly shifting the bands contributing to the spin moment, as will be demonstrated in this paper.

More recent research has required the use of further sophisticated approaches, relying on either molecular orbital methods (GAMESS) or a variety of electronic structure calculations. In $NbFe_2$, comparison with electronic structure calculations for different possible ground states revealed the magnetic order to be ferrimagnetic [19]. Such work shows how electronic structure calculations can be used as the basis for fitting to the data to reveal the pertinent features of the underlying electronic structure, again demonstrating the benefit of not simply relying on purely *ab initio* calculations.

In this paper, we report on recent work that demonstrates the possibility of determining the Fermi level spin polarization in highly spin-polarized materials. We apply the method to Ni, which provides an excellent test of the approach, demonstrating comparison with previous experimental measurements and theory. Our work shows that an accurate determination of the Fermi level spin polarization is indeed possible, and that the band shifting and fitting described above is essential to the technique's success.

## 2. Experimental details and considerations

Magnetic Compton profiles are normally measured on the beam line BL08W at the SPring-8 synchrotron or on ID15 at the ESRF. The SPring-8 facility has a sample environment consisting of a superconducting solenoid to provide the applied magnetic field of up to 2.5T and temperatures down to approximately 6K. An incident X-ray energy of 175keV is normally used. The energy spectrum of the scattered flux is measured using a ten-element Ge detector at a mean scattering angle of 173°, giving a momentum resolution of the magnetic Compton spectrometer, taken as the full-width at half-maximum (FWHM) of the instrument response function, of 0.50 a.u. of momentum (where 1 a.u.=$1.99 \times 10^{-24}\,\mathrm{kg\,m\,s^{-1}}$). At the ESRF, an Oxford Instruments Spectromag cryomagnet is currently used to obtain fields up to 9 tesla. However, the experimental results presented in this paper were collected with a rotating 1 tesla permenent magnet at room temperature. At the ESRF a thirteen-element Ge detector is available. The incident energy of 220keV and scattering angle of 172° result in a 0.44 a.u. resolution. In both experiments, the data need to be corrected for energy-dependent detector efficiency, sample absorption, and the relativistic scattering cross-section. The profiles are then corrected for multiple scattering using the technique described by Felsteiner [20].

## 3. Determination of spin polarization at the Fermi level

The degree of spin polarization at the Fermi level is a measure of the majority and minority density of states (DOS) at this energy. Hence, it contains information concerning the relative contribution to conduction provided by the two spin channels. The degree of spin polarization, $P$, can be defined simply as follows:

$$P = \frac{N_\uparrow - N_\downarrow}{N_\uparrow + N_\downarrow}, \tag{3}$$

where $N_\uparrow$ and $N_\downarrow$ are the spin up and spin down Fermi level densities of states respectively.

Ideally, materials for applications would be fully spin-polarized 'half-metals' (HMs), $P = 1$, where the density of states at the Fermi level is finite for one spin, but zero for the other, such that carriers of only one spin exist at the Fermi level. Such spin-polarized transport is central to the concept of 'spintronics'. In these materials and devices, the goal is to exploit the electron spin for applications such as data storage and read-heads. For example, magnetic random access memory

devices (MRAM) are based on the concept of spin-dependent tunnelling magnetoresistance [21]. Ferromagnets typically have a degree of Fermi level spin-polarization, but in general this is only partial, and not high enough for applications. Only a few promising candidates, such as $CrO_2$ [22, 23], optimally doped $La_{0.7}Sr_{0.3}MnO_3$ [24], $Co_2MnAl_{(1-x)}Sn_x$ [25, 26] and possibly $Co_{(1-x)}Fe_xS_2$ [27, 28, 29, 30] have been found to exhibit high polarizations.

The direct and unambiguous experimental measurement of $P$ is difficult. Techniques such as saturation magnetization or transport measurements can only give an indication of half-metallicity, and techniques which give access to the magnitude of $P$ directly such as spin-polarized photoemission or point-contact Andreev reflection (PCAR) are heavily dependent on the surface quality of the sample. Moreover, the quantity that is actually measured by transport-based probes is weighted by the Fermi velocity. As pointed out by Mazin [31], when comparing such data with theoretical results, the precise definition of $P$ is problematic, resulting in several definitions [31, 32]. In most studies, the polarization is defined in terms of the spin-dependent density of states, $N_{\uparrow/\downarrow}$ at the Fermi level ($E_F$), and the spin-dependent Fermi velocity, $v_{F,\uparrow/\downarrow}$. Following Mazin [31], $P_n$ is defined such that,

$$P_n = \frac{N_\uparrow v_{F,\uparrow}^n - N_\downarrow v_{F,\downarrow}^n}{N_\uparrow v_{F,\uparrow}^n + N_\downarrow v_{F,\downarrow}^n}, \tag{4}$$

where $v_{F,\uparrow/\downarrow}$ is raised to the power of $n$. For $n = 0$, as quoted by most theoretical studies, $P_0$ is solely defined by the DOS. Taking $n = 1$ or $n = 2$, the polarization is weighted with $v_F$ in the ballistic or $v_F^2$ in the diffusive regime. For HMs, $P_n$ is unambiguously 100% while in the case of non-HMs, the values of $P_n$ will generally differ according to the definition adopted. However, the exact weighting of $P_n$ is difficult to extract experimentally and it is thus not clear which regime is appropriate for particular classes of material [33]. Consequently the comparison with other techniques and theory is notoriously difficult [31, 33].

$P_n$ can be calculated directly from band structure calculations, but, as is clear from magnetic Compton scattering measurements such as those on Ni, *ab initio* calculations can have a characteristic difficulty in correctly describing the correct Fermi energy electronic structure. In this paper, we demonstrate a solution to this problem. By performing a rigid-band fit of the calculated MCPs to experiment, we can make an accurate determination of the Fermi level DOS, and it becomes possible to extract $P_n$ for $n = 0$ as well as the weighted values for $n = 1, 2$.

In order to demonstrate this method, the spin polarization of Ni has been calculated and compared with previous experimental [34] and theoretical results [31]. The experimental data gave a spin polarization of $P_2 = 23 \pm 3\%$, using spin-polarized electron tunnelling. Whilst this technique gives excellent results, it relies on high-quality films grown on a superconducting substrate, which is not possible for many materials. For our magnetic Compton scattering approach, experimental data for four crystallographic directions from Dixon *et al.* [16] were used for the fitting procedure. The results of this fitting are shown in Fig. 1. For more details of the method of producing these fitted data, and intracacies involved, see references [17, 18]. It is important to note that several directional MCPs, measured on a single crystal, should be fitted simultaneously in order to have confidence in the optimised DOS and hence $P$ values.

The self-consistent results for the spin polarization $P_n$ are shown in Fig. 2a. Our data agree well with those of Mazin [31]. It can be seen that the calculated value of $P_2$ is 0%, whereas the experimentally determined value from the spin-polarized tunnelling measurements is $23 \pm 3\%$ [34]. Tuning our calculations by fitting the resultant magnetic Compton profiles to the experimental data as shown in Fig. 1, produces the polarization plots shown in Fig. 2b. Here, the fitting had only a small effect on $P_0$ and $P_1$. On the other hand, the fitting increased the value of $P_2$ from 0% to $20 \pm 2\%$. This fitted value compares very well with the previous experimental result. This result demonstrates how the method provides a useful measure of the spin polarization values. Further evidence of the methods efficacy can be seen in the study of the highly spin-polarized

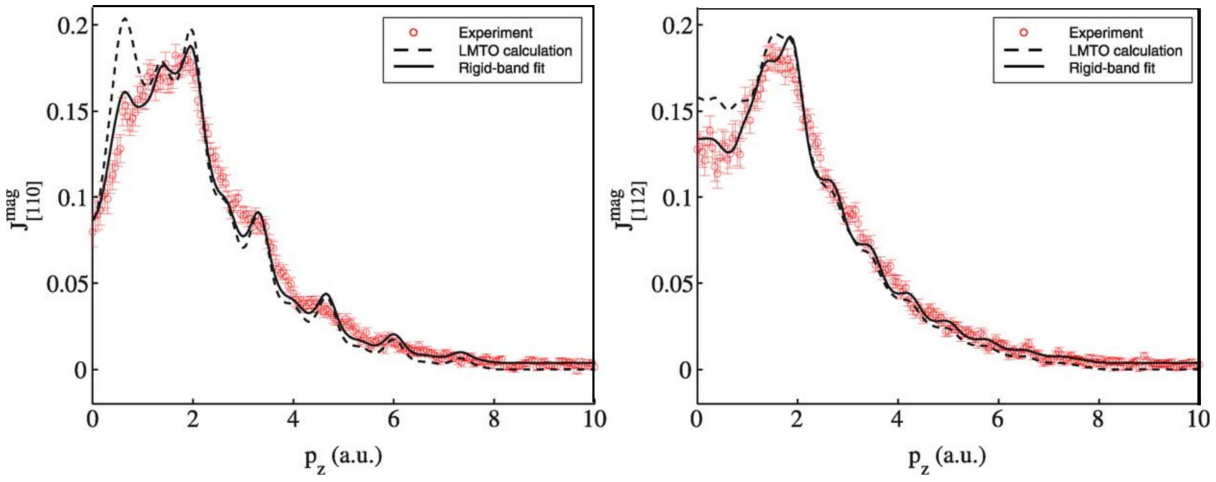


**Figure 1.** The magnetic Compton profiles for Ni, measured along the [100] and [110] directions. Also shown are the results of the raw and tuned calculations. Note that the agreement at low momentum is much better for the fitted band structure.

$Co_{(1-x)}Fe_xS_2$ system [35].

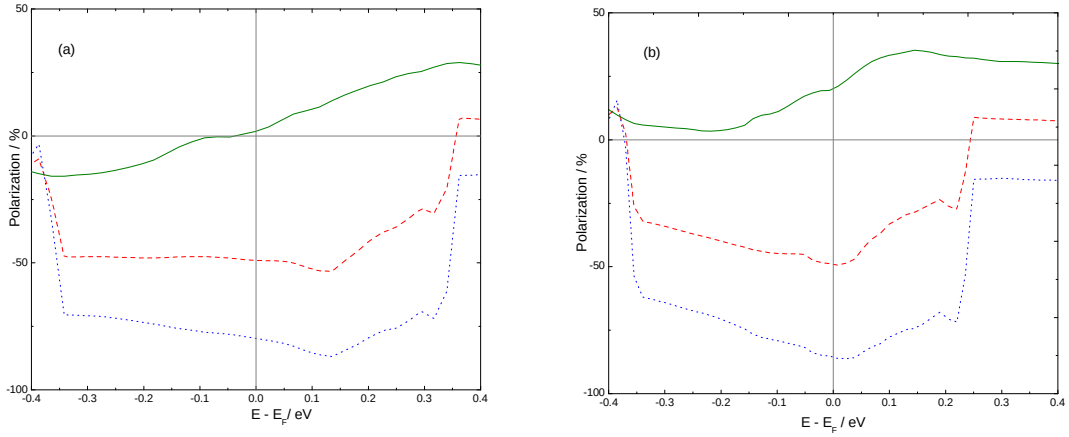


**Figure 2.** The value of the spin polarization across the Fermi level for (a) the raw and (b) the fitted calculations. Results are shown for $P_0$ (blue dots), $P_1$ (red dashes) and $P_2$ (green line). It can be seen that the fitting changes the Fermi level value of $P_2$ from 0% to $20 \pm 2\%$
.

## 4. Outlook

Magnetic Compton scattering has a wide range of applications. Current developments include the improvement of the sample environment available. Our new 'Spectromag' cryomagnet can provide magnetic fields up to 9 tesla, and temperatures down to 1.5K. A newly developed microfurnace insert enables temperatures up to approximately 800K to be obtained. This facility is extending the range of materials that can be studied experimentally.

**Acknowledgments**
I would like to thank many people for their contributions to this research, including C. Utfeld, S.R. Giblin, J. W. Taylor, C. Shenton-Taylor, J. Laverock, S.B. Dugdale, J.E. McCarthy, M.A.G. Dixon and M.J. Cooper. I am grateful for the support of T. Buslaps, V. Honkimaki at the ESRF, and acknowledge the ESRF for providing the beamtime used for the nickel measurements.

**References**
[1] Platzman P M and Tzoar N 1970 *Phys. Rev.* **2** 3556
[2] Holm P 1988 *Phys. Rev. A.* **37** 3706
[3] Sakurai Y *et al.* 2011 *Science* **332** 698
[4] Laverock J *et al.* 2007 *Phys. Rev. B* **76** 052509
[5] Utfeld C *et al.* 2010 *Phys. Rev. B* **81** 064509
[6] Crowe S J *et al.* 2004 *Europhysics Letters* **65** 235
[7] Laverock J *et al.* 2010 *Phys. Rev. B* **82** 125127
[8] Bell F, Felsteiner J and Pitaevskii L P 1996 *Phys. Rev. A.* **53** R1213
[9] Duffy J A 2010 *et al.*, *Phys. Rev. B* **81** 134424
[10] Duffy J A *et al.* 1998 *J. Phys.: Condens. Matter* **10** 10391
[11] Duffy J A *et al.* 2000 *Phys. Rev. B* **61** 14331
[12] Shenton-Taylor C *et al.* 2007 *J. Phys.: Condens. Matter* **19** 186208
[13] Banfield Z F *et al.* 2005 *J. Phys.: Condens. Matter* **17** 5533
[14] McCarthy J E *et al.* 2000 *Phys. Rev. B* **62** R6073
[15] Bebb A M *et al.* 2005 *Phys. Rev. B* **71** 024407
[16] Dixon M A G *et al.* 1998 *J. Phys.: Condens. Matter* **10** 2759
[17] Major Zs *et al.* 2006 *J. Phys. Chem. Sol.* **65**, 2011
[18] Major Zs *et al.* 2004 *Phys. Rev. Lett.* **92**, 107003
[19] Haynes T D *et al.* 2012 *Phys. Rev. B* **85**, 115137
[20] Felsteiner J 1997 private communication
[21] Wolf S A *et al.* 2001 *Science* **294** 1488
[22] Ji Y *et al.* 2001 *Phys. Rev. Lett.* **86** 5585
[23] Parker J A *et al.* 2002 *Phys. Rev. Lett.* **88** 196601
[24] Soulen R J *et al.* 1998 *Science* **282** 85
[25] Fecher G H *et al.* 2005 *J. Phys.: Condens. Matter* **17** 7237
[26] Nakatani T M *et al.* 2007 *J. Appl. Phys.* **102** 033916
[27] Zhao G L, Callaway J and Hayashibara M 1993 *Phys. Rev. B* **48** 15781
[28] Wang L *et al.* 2005 *Phys. Rev. Lett.* **94** 056602
[29] Wang L *et al.* 2006 *Phys. Rev. B* **73** 144402
[30] Leighton C *et al.* 2007 *J. Phys.: Condens. Matter* **19** 315219
[31] Mazin I I 1999 *Phys. Rev. Lett.* **83** 1427
[32] Müller G M *et al.* 2009 *Nat. Mater.* **8** 56
[33] Woods G T *et al.* 2004 *Phys. Rev. B* **70** 054416
[34] Meservey R and Tedrow P M 1994 *Phys. Rep.* **238** 173
[35] Utfeld C *et al.* 2009 *Phys. Rev. Lett.* **103** 226403